



HAL
open science

Multi-sensor imaging of plant stresses: Towards the development of a stress-catalogue

Laury Chaerle, Sándor Lenk, Ilkka Leinonen, Lyn Jones, Dominique van Der Straeten, Claus Buschmann

► **To cite this version:**

Laury Chaerle, Sándor Lenk, Ilkka Leinonen, Lyn Jones, Dominique van Der Straeten, et al.. Multi-sensor imaging of plant stresses: Towards the development of a stress-catalogue. *Biotechnology Journal*, 2009, 4 (8), pp.1152-n/a. 10.1002/biot.200800242 . hal-00495060

HAL Id: hal-00495060

<https://hal.science/hal-00495060>

Submitted on 25 Jun 2010

HAL is a multi-disciplinary open access archive for the deposit and dissemination of scientific research documents, whether they are published or not. The documents may come from teaching and research institutions in France or abroad, or from public or private research centers.

L'archive ouverte pluridisciplinaire **HAL**, est destinée au dépôt et à la diffusion de documents scientifiques de niveau recherche, publiés ou non, émanant des établissements d'enseignement et de recherche français ou étrangers, des laboratoires publics ou privés.



Multi-sensor imaging of plant stresses: Towards the development of a stress-catalogue

Journal:	<i>Biotechnology Journal</i>
Manuscript ID:	BIOT-2008-0242.R2
Wiley - Manuscript type:	Review
Date Submitted by the Author:	19-Mar-2009
Complete List of Authors:	Chaerle, Laury; Ghent University Lenk, Sándor; University of Karlsruhe Leinonen, Ilkka; SCRI Jones, Lyn; SCRI Van Der Straeten, Dominique; University of Ghent Buschmann, Claus; University of Karlsruhe
Keywords:	Fluorescence, Image processing , Re-absorption , Stress, Thermography



Review ((11072 words))**Multi-sensor plant imaging: Towards the development of a stress-catalogue**

Laury Chaerle^{*1}, *Sándor Lenk*^{*2}, *Ilkka Leinonen*^{3,4}, *Hamlyn G. Jones*³, *Dominique Van Der Straeten*¹, *Claus Buschmann*⁵

*These authors contributed equally to this manuscript and are listed alphabetically.

¹ Unit Plant Hormone Signalling and Bio-imaging, Ghent University, Ledeganckstraat 35, B-9000 Gent, Belgium

² Department of Atomic Physics, Budapest University of Technology and Economics, Budafoki út 8., H-1111 Budapest, Hungary

³ Plant Research Unit, Division of Environmental and Applied Biology, School of Life Sciences, University of Dundee at SCRI, Invergowrie, Dundee DD2 5DA, Scotland, UK

⁴ Present address: Department of Meteorology, University of Reading, Earley Gate, PO Box 243, Reading, RG6 6BB, UK

⁵ Botanical Institute II, University of Karlsruhe, D-76128 Karlsruhe, Germany

Keywords: Diagnosis · Fluorescence · Image processing · Re-absorption · Stress · Thermography

Correspondence: Dr. Claus Buschmann, Botanical Institute II, University of Karlsruhe, D-76128 Karlsruhe, Germany
E-mail: claus.buschmann@botanik2.uni-karlsruhe.de
Fax: +49-721-608-4874

Abbreviations: *CCD*, charged coupled device; *Chl*, chlorophyll; *Chl-F*, chlorophyll fluorescence; *LED*, light emitting diode; *PS II*, photosystem II; *SA*, salicylic acid; *SWIR*, short wavelength infra red; *TMV*, tobacco mosaic virus; *UV*, ultraviolet; *VIS*, visible

Abstract

Agricultural production is limited by a wide range of abiotic (e.g. drought, water-logging) and biotic (pests, diseases and weeds) stresses. The impact of these stresses can be minimized by appropriate management actions such as irrigation or chemical pesticide application. However further optimization requires the ability to diagnose and quantify the different stresses at an early stage. Particularly valuable information of plant stress responses is provided by (a) thermal imaging which primarily detects changes in transpiration rate and (b) fluorescence sensing which may indicate functioning of photosynthesis and other physiological processes. These can be supplemented by conventional video imagery for study of growth. An efficient early warning system would need to discriminate between different stressors. Given the wide range of sensors, and the association of specific plant physiological responses with changes at particular wavelengths, this goal seems within reach. This is based on the organization of the individual sensor results in a matrix that identifies specific signatures for multiple types of biotic and abiotic stress. In this paper we first review the diagnostic effectiveness of different individual imaging techniques, and then extend this to the multi-sensor stress-identification approach.

█abstract shortened to 190 words, please check█

1 Introduction

In the 1930s, the term 'stress' was introduced as a human health syndrome by the Canadian medical researcher and endocrinologist of Hungarian origin Hans (János) Selye (1907-1982) [1]. Plant stress is defined as "a significant deviation from the conditions optimal for life" [2]. This definition implies that the occurrence of stress depends on the conditions to which a plant has acclimated. One can distinguish between abiotic (radiation, temperature, water, gases, minerals, mechanical effects) and biotic (induced by micro-organisms, animals, plants, anthropogenic factors) stresses.

In order to properly interpret the causes and effects of the different types of stress, it is usual to study single stresses under controlled conditions. Nevertheless such studies are of only partial relevance to natural conditions because plants are normally exposed to a multitude of interacting concurrent influences. Primary stress responses may be modified both by the acclimation and adaptation of the plants to the previous environmental factors, and by interactions with other organisms. As a further complicating factor the effect or impact of these stresses can vary with the developmental stage of the plant.

Stress does not necessarily need to be lethal. Mild stress conditions can lead to an increased resistance, which will help the plant to react to and overcome a subsequent stress (acquired stress resistance). This positive stress has also been termed 'eustress'. A strong stress may immediately lead to acute damage or later on - when there is not enough resistance - to chronic damage. A damaging stress is also called '-distress' [3].

The importance of biotic and abiotic stresses on plant yield and their impact on agricultural production has been widely recognized. Therefore this subject has received ample attention in the last 20 years, as evidenced by multiple reviews and books with a wide range

1
2
3 of ecophysiological topics [2-13] and others with focus on photosynthesis [14, 15],
4
5 phytochemistry [16, 17] and air pollution [18].
6
7

8 This fact, together with the increasing awareness that stresses associated with global
9
10 anthropogenic factors ('greenhouse effect', 'ozone hole') caused by industrialization may have
11
12 substantial ecological and economic impacts, has led to the emergence of a large body of
13
14 literature on detection of plant stresses and plant responses.
15
16

17 With the increasing pressure on available arable land and water resources, plant stress
18
19 alleviation and avoidance will increase in importance in the near future. There is therefore an
20
21 urgent need to improve techniques for the sensitive early detection, monitoring and diagnosis
22
23 of stress to allow effective management responses. It is essential that the detection methods
24
25 are rapid, non-destructive and low cost. The detection of stress-induced changes of
26
27 physiological parameters is a focus of much recent and current basic and applied plant
28
29 physiological research and a range of instruments have been developed in the past 20 years
30
31 that aim to detect stress effects on plants in a non-contact way. The search for optimal
32
33 imaging-derived stress detection parameters is still ongoing, while the advent of multi-sensor
34
35 detection of a combination of parameters could effectively lead to the identification and
36
37 subsequent remediation of emerging stresses. These aims are an integral part of precision
38
39 agriculture, which strives to limit the inputs of nutrients, pesticides and herbicides by
40
41 matching them to the actual crop needs, which would avoid unnecessary expenditures and
42
43 detrimental impact on the environment and ultimately human health.
44
45
46
47
48
49

50 This review is based on an evaluation of stress detection by a range of imaging techniques
51
52 including thermography and different types of fluorescence imaging that was undertaken in
53
54 the frame of the EU-Research Training Network "STRESSIMAGING" but is extended to
55
56 include a wide range of available information on stress-imaging at the leaf and plant level.
57
58
59 Although we concentrate here on measurements applicable at the leaf- or plant-level the
60

1
2
3 results here should provide a sound basis for interpretation of measurements at the canopy or
4 field scale and for application at larger scales and in precision agriculture approaches. It is
5 worth noting, however, that extension to the canopy or remote-sensing scales may provide yet
6 further opportunities for incorporation of additional information useful for stress diagnosis.
7
8
9
10
11

12 The non-contact detection of stress is largely based on optical measurements of plant
13 temperature (by thermal imaging) and fluorescence emission (for recent reviews: [19, 20]).
14 The latter two signals can be subdivided in spectral ranges by applying multi- or hyper-
15 spectral imaging. Thermography and chlorophyll fluorescence imaging are central in this
16 review since they provide information on two key physiological parameters: transpiration and
17 photosynthesis. In certain circumstances these may be supplemented by conventional digital
18 imagery that allows, for example, measurement of growth. The most useful diagnostic
19 information is obtained when several measured parameters, highlighting a wide range of plant
20 physiological responses, are combined: for example leaf temperature with spectral
21 fluorescence detected at particular wavelength bands. In the following sections, the results
22 obtained with the different imaging techniques will be described first. Thereafter multi-sensor
23 stress imaging will be illustrated, and the stress factors and their induced responses will be
24 summarized in a tabular form: the stress catalogue.
25
26
27
28
29
30
31
32
33
34
35
36
37
38
39
40
41
42
43
44
45
46
47
48
49
50
51
52
53
54
55
56
57
58
59
60

2 Thermography

Canopy or leaf temperature, as measured using thermography (thermal infrared sensing or imaging), provides a powerful monitoring tool for a broad range of plant stresses that affect any aspect of plant water relations. The basis underlying most uses of leaf temperature as a stress detection tool is that leaf temperature is strongly affected by transpiration, which itself is primarily regulated by stomatal conductance, with leaf temperature increasing as transpiration rate decreases [21]. Leaf temperature is a particularly sensitive indicator of changes in stomatal conductance because latent heat loss is a large component of the overall leaf energy balance that determines leaf temperature [22]. **Current thermal camera models commonly have a temperature resolution of 0.1°C which is adequate to reveal transpirational changes or heterogeneity at the leaf surface. Spatial resolution however is rather limited in comparison with the currently available cameras for the visual spectrum, but proved to be sufficient for leaf to plant level monitoring, and can be compensated for by automation approaches in which multiple images are captured.**

At a canopy scale where image pixels may include both leaf and soil, observed temperatures can also change as a result of varying vegetative ground cover, with increasing proportions of soil (as the canopy becomes sparser or as leaves wilt) tending to lead to higher temperatures. An approach to correct the observed average temperatures to better reflect leaf temperatures only has been proposed by [23], while for higher resolution data the image analysis approaches described in [24] can be useful.

The development of methods for stress diagnosis or quantification based on leaf temperature observations under field conditions is complicated by the fact that environmental variables, including air temperature, net radiation absorbed (which is a function of leaf angle), boundary layer resistance (a function of leaf size and wind speed) and air vapor pressure

1
2
3 deficit, all affect leaf temperature. Therefore in the simplest applications, thermal sensing is
4
5 commonly used in a relative mode, with comparisons between known healthy and unknown
6
7 sample plants/crops. The “stress index” approach [25] aimed to normalize results for the
8
9 environmental variation. Further improvements in normalization have been made by the use
10
11 of artificial or theoretical wet and dry references, leading to better “stress indices” [26, 27].
12
13 Where all the relevant environmental variables are known, recent work in the
14
15 STRESSIMAGING project has shown that it is possible to obtain quantitative estimates of
16
17 absolute leaf stomatal conductance from thermal images if appropriate reference temperature
18
19 information is available, or by using energy-balance calculations based on appropriate
20
21 meteorological data [27]. Notwithstanding the adoption of “stress indices”, the association of
22
23 leaf temperature rise with the degree of stress is generally *qualitative* rather than *quantitative*,
24
25 partly because conductance itself is only an indirect indicator of the underlying stress (with
26
27 different responses in different species/cultivars) and partly because the relationship between
28
29 the stress indices and stomatal conductance is also dependent on environmental variables.
30
31
32
33
34
35
36
37
38

39 **Abiotic stress detection**

40
41 As already indicated, many stresses, including especially water deficits, lead to stomatal
42
43 closure. Therefore all such stresses can, in principle, be detected and quantified by thermal
44
45 sensing of stomatal closure, albeit in relative mode [28, 29]. In many cases an observed leaf
46
47 temperature increase can be related to water stress, even though a water deficit may not have
48
49 been the original primary stress (see below). This multiple causation also highlights the
50
51 challenge of identifying particular stress classes.
52
53

54
55 Because drought causes stomatal closure and leaf temperature rise, thermal sensing has
56
57 been of particular interest for many years as a tool for scheduling irrigation [25, 30]. A
58
59 fundamental difficulty in the use of stomatal conductance (and hence of leaf temperature) as a
60

1
2
3 proxy indicator of the causal stress is that the relationship between stomatal conductance and
4
5 leaf water status varies between species. Some plant species minimize the depression of leaf
6
7 water potential as the water supply decreases by stomatal closure, for these so-called
8
9 “isohydric” plants [31] stomatal closure (and hence leaf temperature) is a very good indicator
10
11 of water supply. On the other hand, so called “anisohydric” species do not close their stomata
12
13 until the water deficit is severe; in such cases stomatal closure is not a sensitive indicator of
14
15 water deficit stress (see [32]). Sunflower, most crop plants (e.g. wheat, barley and soybean)
16
17 and the grapevine cultivar ‘Shiraz’ are commonly classified as anisohydric, while maize and
18
19 many temperate trees, together with the grapevine cultivar ‘Grenache’ are typically
20
21 characterized as isohydric [31, 33]. The latter are, given their tight stomatal control, suitable
22
23 for thermal sensing for irrigation control [34].
24
25
26
27
28

29 Thermal sensing can also be used to study the spatial and temporal dynamics of plant
30
31 freezing, due to the local heat generation as tissue water freezes [35]. In addition, the rates of
32
33 water loss from leaves can change in response to atmospheric pollution (e.g. [36]), nutritional
34
35 status [37] and salinity [38]. Other abiotic stresses, such as the uptake of herbicides can also
36
37 be detected by thermal imaging. For example, methylurea herbicide uptake induces a
38
39 temperature increase emerging from the main veins and spreading to finally affect the whole
40
41 leaf [39]. Although this effect was visualized with more contrast by using parallel chlorophyll
42
43 fluorescence (Chl-F) imaging (see below), the clear spatial and temporal pattern of the
44
45 development of the thermal effect adds to the information available from the thermal signal
46
47 and helps to distinguish this from other stresses.
48
49
50
51
52
53
54

55 **Biotic stress detection**

56
57 Leaf temperature has been used as an indicator of several biotic stresses [21, 40-43].
58
59 Local, rapidly expanding increases in leaf temperature develop at tobacco mosaic virus
60

1
2
3 (TMV) infection sites in resistant tobacco, before visual symptoms can be discerned [44].
4
5 This symptom is synchronous with an increase in Chl-F and an increase in UV-excited
6
7 fluorescence (see below). As underlying mechanism, a coincident accumulation of the
8
9 phenolic compound salicylic acid (SA) was revealed which reduced transpiration by its
10
11 known stomatal closing activity. Phenolic compounds typically accumulate during resistance
12
13 responses of plants to pathogens, and multiple reports indicate a reduction in stomatal
14
15 conductance or aperture, pointing at a possibly general mechanism of symptom manifestation.
16
17 Apart from phenolics, other classes of chemicals interfere with stomatal control; these include
18
19 various pathogen toxins [45] such as the fungal toxins which cause (internal) tissue
20
21 degradation, leading to local leaf temperature decreases at early stages of *Cercospora*
22
23 infection in sugar beet [46, 47]. Concomitantly Chl-F was shown to increase (see below). An
24
25 increase of the thermal signal was observed, both at early stages of infection with the
26
27 oomycete *Pseudoperonospora cubensis* causing downy mildew in cucumber [48] and in the
28
29 case of the fungus *Phyllosticta* acting on two tree species [49].
30
31
32
33
34
35

36 Plant surface degradation and leaf cell death is commonly a consequence of certain
37
38 specific or multiple biotic aggressions. Such damage frequently decreases leaf temperature
39
40 locally due to evaporation of leaf water from the damaged tissue. Examples where
41
42 temperature decreases occur include the late stages of TMV infection and upon spontaneous,
43
44 disease-like lesion formation in *Arabidopsis* and tobacco [42, 44]. Similarly, damage by
45
46 mechanical leaf wounding can lead to an immediate temperature increase, followed by a
47
48 localized decrease due to water loss from damaged cells, that progressively disappears again
49
50 upon wound healing [49, 50]. In case of arthropod-induced gall formation a temperature
51
52 decrease has also been described [49].
53
54
55
56

57 As well as being of value for the topical diagnosis and monitoring of local (leaf)
58
59 infections, thermal imaging can also provide information relating to root diseases and rots
60

1
2
3 caused by fungi or oomycetes and for vascular wilts induced by the proliferation of bacteria or
4
5 fungi. This is because these all impact on water uptake and transport, and ultimately result in
6
7 a decrease in transpiration (reviewed in [21]). Toxic compounds absorbed by the root system
8
9 of plants will also gradually affect leaf transpiration [39].
10
11

12 13 14 15 **Diagnostic capability**

16
17 From the above it follows that (especially) single-time point leaf temperature
18
19 measurements by themselves are not usually diagnostic, and normally require some ancillary
20
21 information to determine the precise cause of any observed temperature change. As is
22
23 apparent from the detailed symptoms, especially of the various biotic stresses outlined above,
24
25 additional diagnostic information can be obtained from the temporal and spatial dynamics of
26
27 the temperature changes. In general leaf level-stresses, such as caused by leaf infections, tend
28
29 to induce a (persistent) heterogeneous response pattern, whereas root level stresses evolve
30
31 towards a more homogeneous leaf-level response. The spatial and temporal pattern of the
32
33 stress response can most likely provide a first approach to further discriminate different
34
35 stressors. Dedicated image processing algorithms will enable detection and discrimination of
36
37 (the kinetics of) different patterns.
38
39
40
41
42

43 **3 Fluorescence**

44
45
46
47
48 Leaves emit fluorescence upon absorption of radiation ranging from the UV to the visible;
49
50 however this dissipation typically accounts for only a few percent of the actual energy uptake.
51
52
53 Fluorescence always has a longer wavelength (i.e. lower energy per quantum) than the
54
55 absorbed light (“Stokes-shift”).
56

57
58 **Reliable detection of fluorescence emission requires a homogeneous illumination of the**
59
60 **monitored leaf area(s), implying a dedicated illumination system. As mentioned for**

1
2
3 **thermography, in the case of field measurements, confounding influences from the**
4 **environment (weather conditions, time of day) limit the detectability of stress factors.**
5

6
7
8 Several compounds within leaves fluoresce, and one can distinguish between the most
9
10 important emissions including blue-green fluorescence emitted by cell wall bound ferulic acid
11
12 [51, 52] and red-far red fluorescence emitted by chlorophyll (Chl) *a* in photosystem II [53].
13

14
15 The intensity of fluorescence generally depends on (a) the concentration of the fluorophores,
16
17 (b) the temperature of the leaf, (c) the penetration of the excitation light into the leaf and (d)
18
19 the fluorescence emission from different depths of the leaf. Chlorophyll fluorescence (Chl-F)
20
21 is a particularly powerful probe for investigating activity and integrity of the photosynthetic
22
23 system. The intensity of this Chl-F varies as a function of the various alternative pathways
24
25 which compete with fluorescence for de-excitation of radiant energy absorbed by the Chl
26
27 antenna pigments. These include (e) use of energy to drive photosynthetic electron transport
28
29 (photochemical quenching), and (f) non-radiative de-excitation resulting in heat loss (**non-**
30
31 **photochemical quenching – Nfq**). The magnitude of fluorescence is quenched from its
32
33 maximum (F_m - which occurs when the primary electron acceptor is fully reduced) both by
34
35 increasing photosynthetic electron transport and by non-photochemical quenching (including
36
37 photoinhibition) dependent on pH and xanthophyll de-epoxidation in the thylakoids.
38
39 Parameters such as the efficiency of photosystem II (PS II) and rates of electron transport can
40
41 be readily obtained from F_m together with the minimal fluorescence (F_o) and the steady state
42
43 fluorescence (F_s) and the variable fluorescence ($F_v = F_m - F_o$) using the formulae outlined
44
45 earlier [54, 58].
46
47
48
49
50
51

52
53 Fluorescence images have been used as a tool to detect stress susceptibility in different plants,
54
55 comparing genotypes or mutants [59, 61]. Further reviews on biotic and abiotic stress effects
56
57 as monitored by fluorescence imaging have been presented earlier [61, 70]. Chl-F therefore
58
59 primarily assesses effects on photosynthetic function while UV-fluorescence primarily
60

1
2
3 assesses changes in chemical composition; either of these may be modified by abiotic and
4
5 biotic stresses [71].
6

7 **Abiotic stress detection**

8
9
10 Many environmental stresses affect leaf composition and photosynthesis and can therefore be
11
12 monitored using fluorescence imaging; among the most important are drought and mineral
13
14 nutrition. In addition high light becomes particularly damaging to the photosynthetic
15
16 apparatus when photosynthesis is already inhibited (e.g. as a result of low temperatures or
17
18 drought-induced stomatal closure). The excess light leads to photoinhibitory damage to the
19
20 photosystems – a process that can be readily detected as a decrease in Chl-F [65, 72, 73] and
21
22 as a reduction in maximum quantum yield of PS II (F_v/F_m which was introduced by [54]).
23
24 Importantly, plants under stress display an enhanced sensitivity to photoinhibition. As an
25
26 example, the characteristics of photoinhibition and recovery in relation to cold exposure and
27
28 acclimation have been derived from the differences in maximum quantum yield of PS II
29
30 F_v/F_m , detected from images of Chl-F [74].
31
32
33
34
35

36 Plants have evolved countermeasures to avoid light-induced damage. Increased sun
37
38 exposure of leaves leads to a lower intensity of UV-excited Chl-F [20, 75-77], since UV-
39
40 absorbing substances accumulated in the epidermis shield the Chl-containing mesophyll, and
41
42 thus reduce fluorescence excitation by UV. UV-B treatment was shown to lead to an
43
44 increased blue-green fluorescence [78]. The effect of excess light together with the formation
45
46 of reactive oxygen species could be monitored by a decrease of photosynthesis via Chl-F
47
48 images [79-82].
49
50
51

52
53 The most prevalent abiotic stress under natural conditions is water shortage. Although
54
55 drought can affect photosynthetic rate, this is initially at least, primarily through stomatal
56
57 closure with rather little effect on the activity of the photosystems as measured by F_v/F_m (e.g.
58
59 [83]). Nevertheless drought stress can lead to an increase in blue-green fluorescence, a
60

1
2
3 decrease of Chl-F [75, 84-86] and a decrease of variable Chl-F [87-89]. A particularly useful
4
5 measure of stress is the photochemical yield parameter, which is expressed as $(1 - F_s)/F_m$
6
7 [56]. A decrease in Chl-F and its derived parameters for photochemical quenching, and an
8
9 increase in non-photochemical quenching have been demonstrated in leaves of roses
10
11 undergoing progressive water stress [90].
12
13

14
15 In addition to sufficient water supply, nutrients should be available in a balanced way to
16
17 sustain optimal plant growth. Nitrogen deficiency can be recognized by a higher blue-green
18
19 fluorescence and higher Chl-F at 690 nm [91-93]. Blue-green fluorescence increases because
20
21 of changes in secondary metabolism induced by biotic or abiotic stress [94]; Chl-F at 690 nm
22
23 increases due to a lower Chl content of the leaves, which results in less re-absorption of Chl-F
24
25 (for a review see [95]). Low temperatures and gaseous pollutants can also affect
26
27 photosynthesis and Chl-F emission (e.g. [96, 97]). In addition, inhibition of photosynthesis by
28
29 heavy metal uptake was demonstrated by fluorescence imaging [98]. A decrease of Chl-F as
30
31 detected by photography was taken as an indicator of chilling [59], and upon ozone-induced
32
33 damage of *Brassica* plants and beech trees the maximum quantum yield of PS II F_v/F_m was
34
35 significantly reduced [99, 100]. This was also observed at the cellular level at the very early
36
37 stages of ozone stress [101], and more generally, ozone-damage was detected by an increase
38
39 in the Chl-F [102]. Mechanical damage to plant foliage can be caused by both biotic (e.g.
40
41 insect damage) and abiotic factors (e.g. hail damage), but is commonly caused by wind-
42
43 induced movements leading to tearing damage of leaves. An artificially wounded leaf site first
44
45 displays an increase in fluorescence emission, followed by a decrease to zero fluorescence in
46
47 the regions where the cells were irreversibly damaged and subsequently died [103]. Cells
48
49 proximal to a wound are characterized by a rapid induction of quantum efficiency of PS II
50
51 upon actinic illumination after dark adaptation in *Arabidopsis* plants, revealing the power of
52
53 fluorescence imaging to monitor changes in fluorescence induction kinetics [104].
54
55
56
57
58
59
60

1
2
3 Herbicides which inhibit photosynthetic activity (like DCMU or diuron [= 3-(3,4-
4 dichlorophenyl)-1,1-dimethylurea] and linuron) can be detected by an increase in Chl-F. With
5
6
7 time-lapse imaging of the Chl-F one can follow uptake and degradation of these inhibitors
8
9
10 [39, 61, 105-108]. To assess herbicide efficiency, the effects of multiple compounds can be
11
12 tracked in screening approaches [109].

15 **Biotic stress detection**

16
17 Again, the use of fluorescence for detection of biotic stresses, including both arthropod
18
19 and microbial attacks primarily depends on their effects on photosynthesis, Arthropod
20
21 wounding of leaves, mainly by chewing can lead to reductions in quantum efficiency of PS II
22
23 ([110]; Aldea et al. 2006). The leaf areas around the holes created by caterpillars are
24
25 characterized by a lower PS II activity, as visualized by Chl-F images [111]. Even footsteps of
26
27 herbivore insects can be detected by an increased Chl-F [112]. In other cases, leaves affected
28
29 by mite attack or by the tobacco whitefly can be recognized by the increase of blue
30
31 fluorescence in a characteristic pattern related to the arthropod feeding behavior [65]. The
32
33 response of the plant to localized wounding was monitored by Chl-F imaging as a decrease of
34
35 the plant's photosynthetic activity [79, 80, 82]. Infection of sugar beet plants with root
36
37 nematodes also induced an increase in Chl-F emission [113]. Any factor interfering with root
38
39 water or nutrient uptake can thus potentially be revealed at an early stage by monitoring at
40
41
42
43
44
45
46 leaf level.

47
48 Damage caused by micro-organisms is the second but equally important source of biotic
49
50 plant yield losses. Effects of viruses, bacteria, fungi and oomycetes on plant leaf physiology
51
52 have been visualized with Chl-F imaging. For example, the infection with a virulent strain of
53
54 the bacterium *Pseudomonas syringae* could be monitored by a decrease in the maximum
55
56 quantum yield for PS II F_v / F_m [114-116]. The infection of *Arabidopsis* plants with
57
58 *Pseudomonas syringae* was monitored by Chl-F and the different infection phases by
59
60

1
2
3 analyzing the most contrasting images [117]. **This research highlighted the possibility of**
4 **assessing the relative merit of a wide range of chlorophyll fluorescence parameters**
5 **(including NFQ and Maximum yield of PSII) generated by an elaborate measuring**
6 **protocol. Indications were found that certain parameters could excel in signaling the**
7 **onset of the early stages of stress buildup upon bacterial infection. However, spatial**
8 **variability inherent to measuring conditions and plant material characteristics**
9 **(including illumination heterogeneity linked to heterogeneity in leaf morphology)**
10 **reduced the discriminating power and prevented the derivation of a reliable signature or**
11 **classifier. Thus, it is premature to select a particular fluorescence parameter as a**
12 **signature for a given class of stressors; in-depth research will be needed.**

13
14
15
16
17
18
19
20
21
22
23
24
25
26
27
28
29
30
31
32
33
34
35
36
37
38
39
40
41
42
43
44
45
46
47
48
49
50
51
52
53
54
55
56
57
58
59
60

Virus infection can be followed by means of fluorescence imaging (e.g. infection of Chinese cabbage with turnip yellow mosaic virus: [118]). During the early stages of TMV infection of resistant tobacco (*Nicotiana tabacum*) plants, an increase in Chl-F and blue-green fluorescence could be observed along with the rise of the thermal signal [44, 119]. Thereafter, the blue-green fluorescence remained at a high level, but as cell death progressed, leaf temperature decreased sharply at the infected loci, as did the Chl-F. Photosynthetic damage induced by mosaic viruses in susceptible plants was also detected by a variation in variable Chl-F [120-123]. Systemic infection of pepper mild mottle virus (PMMoV) in tobacco (*Nicotiana benthamiana*) plants could be revealed by Chl-F imaging, as a dynamic increase emanating from the main veins [43].

Fungi are generally considered more damaging to crop yields than viral infections, due to their rapid spread and propagation. An early increase of Chl-F was observed upon infection of sugar beet plants with the fungus *Cercospora* [46, 47]. The decrease of the photosynthetic electron transport upon infection with fungi was demonstrated by Chl-F images representing the photochemical yield parameter $(1 - F_s) / F_m$ (bean plants infected with *Colletotrichum*

1
2
3 *lindemuthianum*: [124]), the maximum quantum yield of PS II F_v / F_m (tomato leaves infected
4 with *Botrytis cinerea*: [125] or barley leaves infected with *Blumeria graminis*: [126]) or $(F'_m -$
5 $F') / F'_m$ (measurements obtained during full-spectrum photosynthetic illumination in tobacco
6 leaves infected with *Phytophthora nicotianae*: [127]). An increase in blue-green fluorescence
7 has been reported in images of grapevine infected with powdery mildew (*Uncinula necator*,
8 [128]). Many fungi exert their damaging effects through the secretion of toxins. The action of
9 these fungal phytotoxins could be visualized by fluorescence imaging [129]. Destruxin (a
10 phytotoxin of the fungus *Alternaria brassica*, which causes significant damage to *Brassica*
11 crops) in a concentration as low as 0.05 mg l^{-1} induced an increase of the imaged Chl-F ratio
12 F_0 / F_m [130]. As a further example, the efficiency of PS II was decreased upon infection of
13 oat leaves with crown rust *Puccinia coronata* [131]. Various phases of infection could be
14 followed by imaging of Chl-F during infection of bean leaves with bean rust (*Uromyces*
15 *appendiculatus*) [132].

16
17
18
19
20
21
22
23
24
25
26
27
28
29
30
31
32
33
34
35
36
37
38
39
40
41
42
43
44
45
46
47
48
49
50
51
52
53
54
55
56
57
58
59
60
In an agricultural context, some plants are considered pests since they compete with the
cultivated crops. Chl-F imaging can be advantageously used to visualize the speed of
herbicide uptake and to quantify its effects. The penetration of the herbicide diuron, which
inhibits PS II activity, can be followed in a time-lapse sequence of fluorescence images,
showing the increase of Chl-F in the affected leaf tissue [106].

Diagnostic capability

As pointed out above for thermal imaging, the physiological processes (especially
photosynthesis) detected by fluorescence are potentially affected by a wide range of biotic and
abiotic stresses. An explorative approach in which multiple chlorophyll fluorescence imaging
derived parameters are quantified and plotted according to a spider diagram provide a visual
signature of the stress impact and have the potential for automated recognition [115, 117]. For
comparative purposes different stressors have to be measured according to the same

1
2
3 measuring protocol and under similar conditions to be able to draw conclusions and to expand
4
5 on the preliminary stress class classification of Table1. In addition effective methods for
6
7 distinguishing between different causes of the symptoms detected again depend on both the
8
9 utilization of the temporal and spatial characteristics of the response and the use of
10
11 complementary signals (such as thermal imagery, blue-green fluorescence and reflectance
12
13 indices) that respond to different physiological processes. **A combination of temporal**
14
15 **measurements and multiple imaging techniques likely will allow to derive time-**
16
17 **dependent signatures typical for a particular stress factor, and provide enough**
18
19 **redundancy to overcome the confounding effects of measuring conditions.**
20
21
22
23
24
25
26
27
28
29
30
31
32
33
34
35
36
37
38
39
40
41
42
43
44
45
46
47
48
49
50
51
52
53
54
55
56
57
58
59
60

4 Future development: Multi-sensor monitoring

With the ongoing technical development, imaging is more and more replacing the usual point measurement devices. Imaging allows measuring multiple samples (plants, leaves or leaf regions) simultaneously with a high two-dimensional resolution, and thus provides both the statistical distribution of the signal and information on the spatial variation. The use of imaging lends itself to a multi-sensor approach where images are obtained using different sensors (thermal and fluorescence) and overlaid to obtain a wide range of information for each area of the object. This maximizes the opportunities for discriminating stresses. A promising technique in this respect seems also the 'combinatorial imaging' by searching the most contrasting images taken with different protocols, **as illustrated for chlorophyll fluorescence parameters [117] , and the analysis of time sequence images [133]. The latter is advantageously combined with the derivation of parameters describing image statistical information, for example maximum temperature difference (MTD) as a measure of heterogeneity in thermal images [48]. A similar approach can be applied to chlorophyll fluorescence (parameter) images. Developing strategies of signature definition and recognition based on dedicated models and training datasets is gaining importance as an approach for stress factor discrimination [115], [19 and references therein].**

When considering field or greenhouse measurements, adequate monitoring of environmental data is of prime importance to ascertain comparability of the obtained data to earlier or future results. The same pertains to closed environment measurements when considering integration of results obtained by different research groups on monitoring multiple plant-stressor combinations into a global overview that aims at a first-line identification of stressor classes.

Thermal imaging

Thermography detects infrared radiation within the 3 to 14 micrometer range, the exact wavelength sensitivity depending on the chosen model, and can readily reveal temperature distributions at plant canopy to leaf level, without the need for any illumination. Many current models have a sensitivity of 0.1 °C which is adequate for leaf temperature heterogeneity visualization. Thermal cameras are increasingly popular with industrial, maintenance and safety monitoring, which tends to further lower their price **and increases the availability of higher resolution detectors.**

Fluorescence imaging

A fluorescence imaging system includes an excitation light source(s), a detector equipped to measure only at specific wavebands (usually achieved by inserting filter(s) in front of the camera), and a computer for controlling the measurement, the data acquisition and the data analysis (see e.g. [66]). **The excitation light distribution over the target surface needs to be as homogeneous as possible to avoid masking the heterogeneity of the photosynthetic processes underlying the chlorophyll fluorescence emission.**

The spectral range of the excitation light source determines the fluorescence that can be measured. When measuring Chl-F blue or short wavelength red excitation is used most frequently, because Chls absorb in these regions with the highest quantum efficiency. With UV radiation both blue-green fluorescence and Chl-F can be detected. However, when using UV excitation the intensity of Chl-F strongly depends on the presence of UV absorbing substances in the epidermis which cause UV shielding of the Chl in the mesophyll tissue below.

The light sources are usually operated in pulsed mode in order to eliminate ambient and reflected background light. As light sources either light emitting diodes (LEDs) or lamps

1
2
3 (Xenon or halogen) fitted with band-pass filters are used. The fluorescence images are
4
5 detected by monochrome charged coupled device (CCD) cameras combined with different
6
7 band-pass filters (e.g. a high-pass red filter blocking all light with wavelength smaller than
8
9 650 nm for Chl-F detection) and synchronized with the excitation light pulses. Cooled CCDs
10
11 are used for the determination of particularly low fluorescence signals (e.g. F_0) [67]. CCDs
12
13 with an image intensifier unit allow shorter integration time, and photon counting for
14
15 measuring extremely short and low signals, respectively.
16
17
18

19
20 When using imaging to monitor stress responses, it is beneficial to compare several
21
22 repeats and treatments or cultivars with differing resistance levels within a single experiment.
23
24 Either high-resolution sensors or automation can accommodate screening approaches. The
25
26 latter setup can be realized by robotized systems that move the sensor, or alternatively the
27
28 plants.
29
30

31
32 Manual analysis of many images is generally time consuming, and especially with thermal
33
34 images it is often difficult to separate leaf area from background. To solve these problems, a
35
36 semi-automated method for image analysis was developed [24]. In this method, information
37
38 from images of different type is combined to identify the area of interest. First, two different
39
40 images (e.g. thermal and visible or thermal and fluorescence) representing the same area are
41
42 overlaid using pre-selected reference (or “ground control”) points. Second, the leaf area is
43
44 separated from background using for example supervised classification for the visible image
45
46 or pixel intensity thresholding in the fluorescence image. Finally, the identified leaf area is
47
48 used to extract leaf-specific information from the other image, for example to calculate the
49
50 temperature statistics of leaves in the thermal image. In cases where the positions of the
51
52 cameras (thermal, fluorescence) are fixed in relation to each other [46], the method can be
53
54 fully automated and allows rapid analysis of large number of images. In addition, specific
55
56
57
58
59
60

1
2
3 masks can be obtained for discriminating shadow versus sunlit leaves under field conditions
4
5 [134].
6
7

8 As described above, although the individual imaging techniques are able to reveal
9
10 symptoms at early stages for a wide range of stresses effective discrimination between causal
11
12 stresses is improved by the use of multiple sensors (such as thermography and chlorophyll
13
14 fluorescence imaging) that monitor different physiological processes. For example both water
15
16 stress and nitrogen deficiency can reduce the Chl concentration (which is revealed by changes
17
18 in Chl-F Imaging), but water stress typically has a more pronounced and swift effect on
19
20 stomatal closure (detected by thermography), given the fact that only water stress leads to leaf
21
22 wilting. Water stress will also inhibit photosynthesis by stomatal limitation of CO₂ uptake,
23
24 which will affect Chl-F emission. As a consequence the kinetics of Chl-F emission will likely
25
26 differ between water stress and nitrogen deficiency.
27
28
29
30
31
32
33

34 **Examples for multi-sensor imaging**

35
36 Dynamics of stomatal patchiness, induced by changes in environmental factors, were
37
38 visualized simultaneously by thermal and chlorophyll fluorescence imaging. [135]. Both
39
40 techniques provide spatial information for the interpretation of heterogeneity of stomatal and
41
42 possibly linked photosynthetic responses, as well as of excess light energy dissipation
43
44 mechanisms [136].
45
46
47

48 Both a viral (TMV) and a fungal (*Cercospora*) infection lead to the enhancement of Chl-F
49
50 emission, followed by a subsequent decrease. The thermal picture shows a marked contrast in
51
52 response, revealing a temperature increase after viral ingress in tobacco, versus a strong local
53
54 cooling for the fungal infection in sugar beet (see Fig. 1). Fungal *Botrytis cinerea* infection in
55
56 common bean resulted in a similar pattern for thermal and chlorophyll fluorescence as
57
58 compared to the viral infection example mentioned above [103]. However, UV-excited
59
60

1
2
3 fluorescence would likely be able to discern these two plant-pathogen interactions, based on
4 the specificity of accumulating fluorescing compounds upon TMV-infection [119]. The 3
5 examples from Figure 1 illustrate that both thermography and Chl-F imaging reveal the
6 infection at an early stage, with Chl-F imaging providing a higher spatial resolution, while
7 thermography visualizes a slightly more extended affected region.
8
9

10
11
12
13
14
15 The quantification of stress-induced tissue damage can be dramatically enhanced by
16 choosing a different imaging sensor or waveband. In general, Chl-F provides excellent
17 contrast in comparison with visual images. Under certain circumstances, however, green
18 fluorescence imaging after UV-excitation proves superior in revealing damage due to its
19 ability to detect specific highly fluorescing compounds induced by a particular stress. In
20 Figure 2, spontaneous cell death is apparent in the visual image of Arabidopsis *lsd* mutants,
21 but thresholding the symptoms from the green fluorescence resolves the symptoms better
22 from the unaffected leaf areas, whereas the chlorophyll fluorescence image displays very little
23 contrast and suffers from signal emission from the background owing to algal growth on the
24 substrate. The affected area calculated per *lsd* plant, by taking the ratio of the 2 thresholded
25 images (green fluorescence over green channel of the visual reflectance image), is 11 and
26 12%, respectively.
27
28
29
30
31
32
33
34
35
36
37
38
39
40
41
42

43 An optimal sensor-combination for discriminating a set of stresses can be chosen on the
44 basis of a thorough understanding of the various physiological causes and effects of each
45 stress. Key responses are summarized in Table 1 which represents the basis for a stress-
46 catalogue.
47
48
49
50
51
52
53
54
55
56
57
58
59
60

5 Conclusion

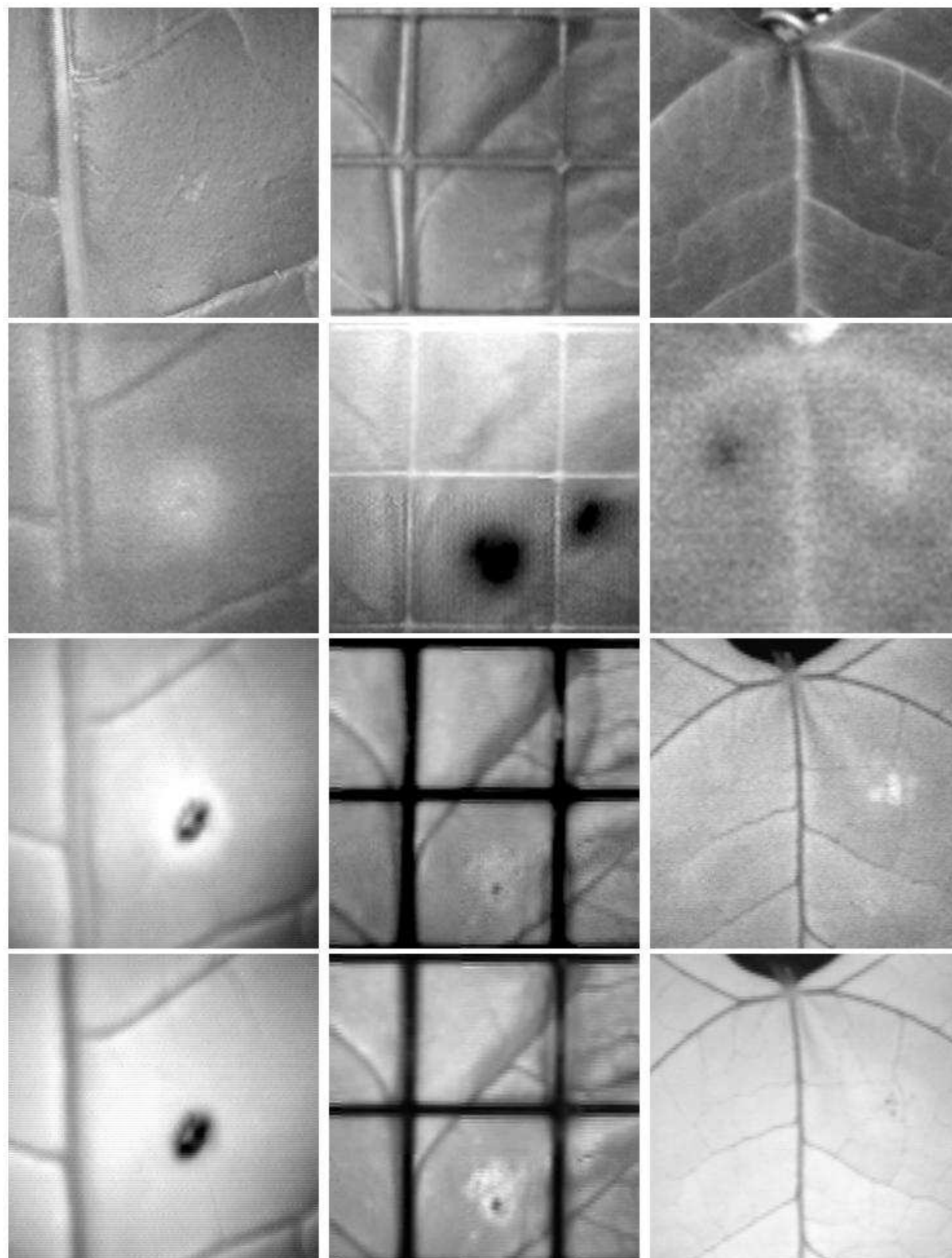
The multi-sensor imaging equipment can be used as a first early-warning system to pick up signals of plants in stress. As a consequence of its mobility that allows a wide range of action, especially in a horticultural or agricultural setting, an imaging sensor will detect emerging stresses, and at the same time allow targeted sampling for further diagnosis. With the aid of a stress catalogue, based on previously established stress responses under controlled or standard conditions (Table 1), a first coarse identification of the stress class will be facilitated. **The stress catalogue will however need to be linked to a performant knowledge model or expert system that makes optimal usage of the sensor fusion approach, to derive the specific signatures needed for a sufficient level of discrimination.** As a next step, the stressor can be identified by using tissue analysis (nutrient deficiencies) or diagnostic tests (pathogens). Therefore the multi-sensor approach could lead to a timely, localized and specific treatment, benefiting both culture economics and the environment and will become a valuable tool for the near future.

Acknowledgements

The work described here was funded by the European Commission through a Research Training Network (STRESSIMAGING), contract HPRN-CT-2002-00254.

S.L. was a junior researcher at the Botanical Institute II, University of Karlsruhe, D-76128 Karlsruhe, Germany

For Peer Review



57 **Figure 1.** Comparison of presymptomatic symptoms of 3 plant pathogen interactions. Each
58 column displays from top to bottom visual color image, thermal image and chlorophyll
59 fluorescence image at respectively low and high excitation intensity.
60

1
2
3 Left column: 54 hours after infection, the TMV-tobacco (*Nicotiana tabacum*) interaction
4 results in a local temperature increase of maximum 0.5°C above the non-affected area of the
5 leaf (corresponding with a 2 fold increase in pixel intensity) (second row). The increase
6 extends beyond the visually affected area (image first row). The area of chlorophyll
7 fluorescence decrease is also more extended than the visual damage, and expanding further
8 outward is a halo of increased fluorescence (third row, halo presents an 1.5 fold increase in
9 pixel intensity compared to unaffected tissue). Chlorophyll fluorescence under high intensity
10 illumination only show the extent of tissue death (fourth row) (see also [46]).
11
12

13
14
15 Middle column: *Cercospora beticola* infection of sugar beet (*Beta vulgaris*) at 7days after
16 infection shows a local decrease in leaf temperature of maximum 1°C (second row), while the
17 visual effect is limited to a pin-point lesion (first row), which can also be seen as a small spot
18 of lower chlorophyll fluorescence (third row). An increase in chlorophyll fluorescence is
19 visible around this spot, and is more clearly visible at higher intensity illumination (fourth
20 row); chlorophyll fluorescence intensity increases at least 3 fold compared with the unaffected
21 leaf area (see also [46]).
22
23

24
25
26 Right column: *Botrytis cinerea* infection of common bean (*Phaseolus vulgaris*) 21 h after
27 infection. An increase in local, leaf temperature is apparent (second row, maximum increase
28 of 0.3°C), while a few co-located spots of increased chlorophyll fluorescence are detectable
29 (third row, intensity increase 2 fold over unaffected tissue). As a reference a wounding spot is
30 included on the other side of the main leaf vein, and visible as a cold spot in the thermal
31 picture (second row). The visible damage (first row) corresponds to the black spots in the Chl-
32 F image captured at high light-intensity (fourth row) (see also [103]).
33
34
35
36
37
38
39
40
41
42
43
44
45
46
47
48
49
50
51
52
53
54
55
56
57
58
59
60

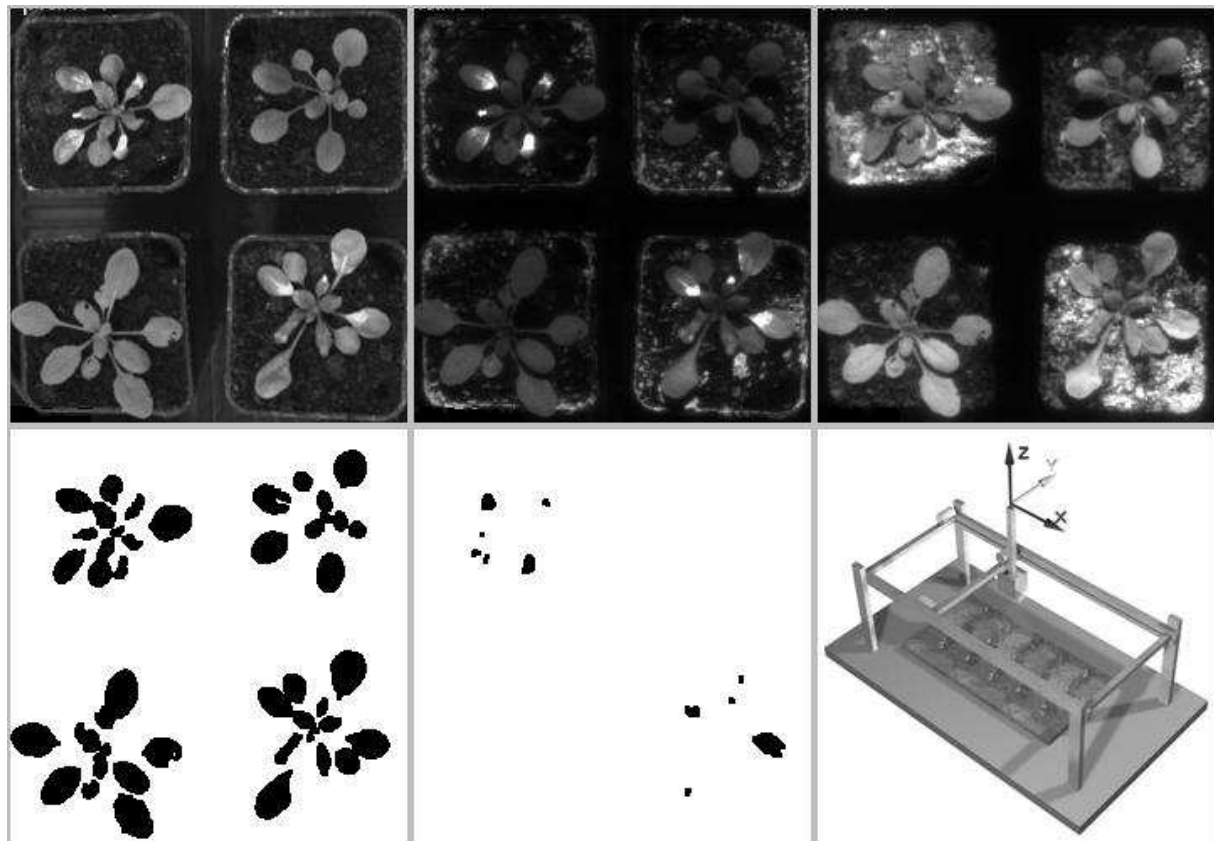


Figure 2. *Arabidopsis* plants as imaged with a multispectral fluorescence imaging system. In each panel, upper left and lower right position feature a spontaneous cell death mutant *Isd* (lesions simulating disease resistance, [42]; the other 2 plants are the Col-0 wild type from which this mutant was derived. Upper left: color reflectance image, middle panel: green fluorescence emission (550nm), right panel: chlorophyll fluorescence emission (690nm). The lower panels show thresholding of respectively color video and green fluorescence image, the latter indicating the leaf area affected by cell death. Thresholding of the chlorophyll fluorescence image includes part of the growing medium background and displays little or no contrast between affected and unaffected leaf areas, as is already evident from the depicted original fluorescence image. The lower right panel shows a schematic robotized system applicable for multi-sensor imaging.

Tables

For Peer Review

1
2
3
4
5
6
7
8
9
10
11
12
13
14
15
16
17
18
19
20
21
22
23
24
25
26
27
28
29
30
31
32
33
34
35
36
37
38
39
40
41
42
43
44
45
46
47
48
49
50
51
52
53
54
55
56
57
58
59
60

Table 1. Summary of stress effects and their detection by thermography and fluorescence imaging.

	<i>Thermography</i>		<i>Fluorescence</i>	
<i>Abiotic stress</i>				
Water stress	Temperature rise (primary response in 'isohydric plants)	[26, 30]	Increase in blue-green-F, decrease of Chl-F, decrease of variable Chl-F, increase of non-photochemical quenching	[75, 84-90, 137]
Sun exposure			Decrease of UV-excited Chl-F, increase of blue-green fluorescence, detection of reactive oxygen species via fluorescence dyes	[75, 76, 78, 138]
Photoinhibition			Decrease of Chl -F, decrease of variable fluorescence, detection of reactive oxygen species via fluorescence dyes	[65, 73, 74, 138, 139]
Photooxidation			Decrease of photosynthetic electron transport detected by Chl-F, detection of reactive oxygen species via fluorescent dyes	[79-81]
Heavy metal uptake			Decrease of photosynthetic electron transport detected by Chl-F	[98]
Salinity stress	Rise (not consistent)	[40]		
Freezing	Rise (freezing exotherm)	[35]		
Chilling			Decrease of variable Chl-F	[139]
Nitrogen deficiency	Tendency to rise (may relate to the reduced leaf area effect)	[40]	Higher blue-green-F and higher Chl-F at 690 nm	[91, 93]
Gaseous pollutants (NO ₂ , SO ₂ , O ₃)	Rise (result of stomatal closure with often increased stomatal heterogeneity)	[36, 96, 97]	Chl-F increase	[99, 102]
Wounding	Temperature decrease due to water loss	[50, 140]	Decrease of photosynthetic electron transport detected by Chl-F, rapid induction of quantum efficiency of photosystem II	[79, 80, 82, 104]
Herbicides	Temperature increase	[39]	Diuron or linuron: increase of Chl-F	[39, 61, 102, 105-108]
<i>Biotic stress</i>				
Insect attack			Increase of blue-F, change of photosynthetic parameters	[65, 110, 111]

			derived from Chl-F images	
Vascular wilt diseases and root rots	Raise temperatures as lead to water deficits and stomatal closure	[40]		
Fungal foliar infection	Temperature decrease	[46, 48]	Increase of Chl-F decrease of variable Chl-F, increase of blue-green-F	[132]; [131]; [124]; [130]; [125];[46];[127];[126];[128]
Viral infection	TMV: Initial temperature rise, follo-wed by decrease upon cell death	[44]	Variation in Chl-F parameters related to photosynthesis, increase of Chl-F and blue-green-F	[43, 118, 121-123]
Bacterial infection	<i>Erwinia</i> : Presymptomatic temperature decrease	[141]	decrease of variable fluorescence	[114-117]

1
2
3
4
5
6
7
8
9
10
11
12
13
14
15
16
17
18
19
20
21
22
23
24
25
26
27
28
29
30
31
32
33
34
35
36
37
38
39
40
41
42
43
44
45
46
47

References

- [1] Selye, H., *The Stress of Life*, Mc Graw Hill, New York 1956.
- [2] Larcher, W., *Physiological Plant Ecology: Ecophysiology and Stress Physiology of Functional Groups*, Springer, Berlin 2003.
- [3] Lichtenthaler, H. K. (Ed.), *Vegetation Stress*, G. Fischer, Stuttgart 1995.
- [4] Hale, M. G., Orcutt, D.M. (Ed.), *The Physiology of Plants under Stress*, Wiley, New York 1987.
- [5] Tenhunen, J. D., Catarino, F.M., Lange, O.L., Oechel, W.C. (Ed.), *Plant response to stress: Functional analysis in Mediterranean ecosystems*, Springer, Berlin 1987.
- [6] Jones, H. G. (Ed.), *Plants under Stress: Biochemistry, Physiology and Ecology and their Application to Plant Improvement*, Cambridge University Press 1989.
- [7] Alscher, R. G., Cumming, J.R. (Ed.), *Stress Responses in Plants: Adaptation and Acclimation Mechanisms*, Wiley-Liss, New-York 1990.
- [8] Fowden, L. (Ed.), *Plant Adaptation to Environmental Stress*, Chapman & Hall, London 1993.
- [9] Brunold, C. (Ed.), *Stress bei Pflanzen: Ökologie, Physiologie, Biochemie, Molekularbiologie*, Haupt, Bern 1996.
- [10] Csermely, P. (Ed.), *Stress of Life: From Molecules to Man*, New York Academy of Sciences, New York 1998.
- [11] Lerner, H. R. (Ed.), *Plant Responses to Environmental Stress: From Phytohormones to Genome Reorganization*, Marcel Dekker, New York 1999.

- 1
2
3
4
5
6 [12] Smallwood, M. F., Calvert, C.M., Bowles, D.J. (Ed.), *Plant Responses to*
7
8 *Environmental Stress*, BIOS Scientific, Oxford 1999.
9
- 10 [13] Yunus, M. (Ed.), *Environmental Stress: Indication, Mitigation, and Eco-*
11
12 *conservation*, Kluwer, Dordrecht 2000.
13
- 14 [14] Marcelle, R. (Ed.), *Effects of Stress on Photosynthesis*, Nijhoff, The Hague
15
16
17 1983.
18
- 19 [15] Satoh, K., Murata, N.K. (Ed.), *Stress Responses of Photosynthetic*
20
21 *Organisms: Molecular Mechanisms and Molecular Regulations*, Elsevier,
22
23
24
25
26 Amsterdam 1998.
- 27 [16] Timmermann, B. N. (Ed.), *Phytochemical Adaptations to Stress*, Plenum
28
29
30 Press, New York 1984.
- 31 [17] Cherry, J. H. (Ed.), *Environmental Stress in Plants: Biochemical and*
32
33 *Physiological Mechanisms*, Springer, Berlin 1989.
34
- 35 [18] Treshow, M., Anderson, F.K., *Plant Stress from Air Pollution*, Wiley,
36
37
38
39 Chichester 1989.
- 40 [19] Chaerle, L., Leinonen, I., Jones, H. G., Van Der Straeten, D., Monitoring and
41
42
43 screening plant populations with combined thermal and chlorophyll fluorescence
44
45
46 imaging. *J. Exp. Bot.* 2007, 58, 773-784.
47
- 48 [20] Lenk, S., Chaerle, L., Pfundel, E. E., Langsdorf, G., *et al.*, Multispectral
49
50
51 fluorescence and reflectance imaging at the leaf level and its possible applications.
52
53
54 *J. Exp. Bot.* 2007, 58, 807-814.
- 55 [21] Jones, H. G., Application of thermal imaging and infrared sensing in plant
56
57
58 physiology and ecophysiology. *Adv. Bot. Res.* 2004, 41, 107-163.
59
60

- 1
2
3
4
5
6 [22] Jones, H. G., *Plants and Microclimate : a Quantitative Approach to*
7
8 *Environmental Plant Physiology*, Cambridge university press, Cambridge 1992.
9
10 [23] Moran, M. S., Clarke, T. R., Inoue, Y., Vidal, A., Estimating crop water
11
12 deficit using the relation between surface-air temperature and spectral vegetation
13
14 index. *Remote Sens. Environ.* 1994, 49, 246-263.
15
16
17 [24] Leinonen, I., Jones, H. G., Combining thermal and visible imagery for
18
19 estimating canopy temperature and identifying plant stress. *J. Exp. Bot.* 2004, 55,
20
21 1423-1431.
22
23
24 [25] Idso, S. B., Jackson, R. D., Pinter, P. J., Reginato, R. J., Hatfield, J. L.,
25
26 Normalizing the stress-degree-day parameter for environmental variability. *Agr.*
27
28 *Meteorol.* 1981, 24, 45-55.
29
30
31 [26] Jones, H. G., Use of thermography for quantitative studies of spatial and
32
33 temporal variation of stomatal conductance over leaf surfaces. *Plant Cell Environ.*
34
35 1999, 22, 1043-1055.
36
37
38 [27] Leinonen, I., Grant, O. M., Tagliavia, C. P. P., Chaves, M. M., Jones, H. G.,
39
40 Estimating stomatal conductance with thermal imagery. *Plant Cell Environ.* 2006,
41
42 29, 1508-1518.
43
44
45 [28] Chaerle, L., Saibo, N., Van Der Straeten, D., Tuning the pores: towards
46
47 engineering plants for improved water use efficiency. *Trends Biotechnol.* 2005,
48
49 23, 308-315.
50
51
52 [29] Grant, O. M., Chaves, M. M., Jones, H. G., Optimizing thermal imaging as a
53
54 technique for detecting stomatal closure induced by drought stress under
55
56 greenhouse conditions. *Physiol. Plant.* 2006, 127, 507-518.
57
58
59
60

- 1
2
3
4
5
6 [30] Jones, H. G., Irrigation scheduling: advantages and pitfalls of plant-based
7
8 methods. *J. Exp. Bot.* 2004, 55, 2427-2436.
9
- 10 [31] Tardieu, F., Simonneau, T., Variability among species of stomatal control
11
12 under fluctuating soil water status and evaporative demand: modelling isohydric
13
14 and anisohydric behaviours. *J. Exp. Bot.* 1998, 49, 419-432.
15
16
- 17 [32] Jones, H. G., Irrigation scheduling - Comparison of soil, plant and
18
19 atmosphere monitoring approaches *Acta Hort. (ISHS)* 2008, 391-403.
20
21
- 22 [33] Schultz, H. R., Differences in hydraulic architecture account for near-
23
24 isohydric and anisohydric behaviour of two field-grown *Vitis vinifera* L. cultivars
25
26 during drought. *Plant Cell Environ.* 2003, 26, 1393-1405.
27
28
- 29 [34] Chaerle, L., Van Der Straeten, D., Regulating plant water status by stomatal
30
31 control, in: Jenks, M. A., Hasegawa, P.M., Mohan Jain, S. (Ed.), *Advances in*
32
33 *Molecular Breeding Toward Drought and Salt Tolerant Crops*, Springer
34
35 Netherlands 2007, pp. 73-90.
36
37
- 38 [35] Fuller, M. P., Wisniewski, M., The use of infrared thermal imaging in the
39
40 study of ice nucleation and freezing of plants. *J. Therm. Biol.* 1998, 23, 81-89.
41
42
- 43 [36] Omasa, K., Hashimoto, Y., Aiga, I., Image instrumentation of plants exposed
44
45 to air pollutants I. Quantification of physiological information included in thermal
46
47 infrared image. *Res. Rep. Nat. Inst. Environ. Stud.* 1984, 66.
48
49
- 50 [37] Wakiyama, Y., Infrared remote sensing of canopy temperature in paddy field
51
52 and relationship between leaf temperature and leaf color. *J. Agr. Meteorol.* 2002,
53
54 58, 185-194.
55
56
57
58
59
60

- 1
2
3
4
5
6 [38] Sharma, S., Soil salinity effects on transpiration and net photosynthetic rates,
7 stomatal conductance and Na⁺ and Cl⁻ contents in durum wheat. *Biol. plant.*
8 1996, 38, 519-523.
9
10 [39] Chaerle, L., Hulsen, K., Hermans, C., Strasser, R. J., *et al.*, Robotized time-
11 lapse imaging to assess in-planta uptake of phenylurea herbicides and their
12 microbial degradation. *Physiol. Plant.* 2003, 118, 613-619.
13
14 [40] Nilsson, H. E., Remote sensing and image analysis in plant pathology. *Annu.*
15 *Rev. Phytopathol.* 1995, 33, 489-527.
16
17 [41] Chaerle, L., Van Der Straeten, D., Imaging techniques and the early detection
18 of plant stress. *Trends Plant Sci.* 2000, 5, 495-501.
19
20 [42] Chaerle, L., De Boever, F., Van Montagu, M., Van Der Straeten, D.,
21 Thermographic visualisation of cell death in tobacco and *Arabidopsis*. *Plant Cell*
22 *Environ.* 2001, 24, 15-26.
23
24 [43] Chaerle, L., Pineda, M., Romero-Aranda, R., Van Der Straeten, D., Barón,
25 M., Robotized thermal and chlorophyll fluorescence imaging of pepper mild
26 mottle virus infection in *Nicotiana benthamiana*. *Plant Cell Physiol.* 2006, 47,
27 1323-1336.
28
29 [44] Chaerle, L., Van Caeneghem, W., Messens, E., Lambers, H., *et al.*,
30 Presymptomatic visualization of plant-virus interactions by thermography. *Nature*
31 *Biotechnol.* 1999, 17, 813-816.
32
33 [45] Chaerle, L., Van Der Straeten, D., Seeing is believing: imaging techniques to
34 monitor plant health. *Biochim. Biophys. Acta-Gene Struct. Express.* 2001, 1519,
35 153-166.
36
37
38
39
40
41
42
43
44
45
46
47
48
49
50
51
52
53
54
55
56
57
58
59
60

- 1
2
3
4
5
6 [46] Chaerle, L., Hagenbeek, D., De Bruyne, E., Valcke, R., Van Der Straeten, D.,
7
8 Thermal and chlorophyll-fluorescence imaging distinguish plant-pathogen
9
10 interactions at an early stage. *Plant Cell Physiol.* 2004, *45*, 887-896.
11
12 [47] Chaerle, L., Hagenbeek, D., De Bruyne, E., Van Der Straeten, D.,
13
14 Chlorophyll fluorescence imaging for disease-resistance screening of sugar beet.
15
16 *Plant Cell Tissue Organ Cult.* 2007, *91*, 97-106.
17
18 [48] Oerke, E. C., Steiner, U., Dehne, H. W., Lindenthal, M., Thermal imaging of
19
20 cucumber leaves affected by downy mildew and environmental conditions. *J. Exp.*
21
22 *Bot.* 2006, *57*, 2121-2132.
23
24 [49] Aldea, M., Hamilton, J. G., Resti, J. P., Zangerl, A. R., *et al.*, Comparison of
25
26 photosynthetic damage from arthropod herbivory and pathogen infection in
27
28 understory hardwood saplings. *Oecologia* 2006, *149*, 221-232.
29
30 [50] Chaerle, L., De Boever, F., Van Der Straeten, D., Infrared detection of early
31
32 biotic stress in plants. *Thermology International* 2002, *12*, 100-106.
33
34 [51] Morales, F., Cerovic, Z. G., Moya, I., Time-resolved blue-green fluorescence
35
36 of sugar beet (*Beta vulgaris* L) leaves. Spectroscopic evidence for the presence of
37
38 ferulic acid as the main fluorophore of the epidermis. *Biochim. Biophys. Acta-*
39
40 *Bioenerg.* 1996, *1273*, 251-262.
41
42 [52] Lichtenthaler, H. K., Schweiger, J., Cell wall bound ferulic acid, the major
43
44 substance of the blue-green fluorescence emission of plants. *J. Plant Physiol.*
45
46 1998, *152*, 272-282.
47
48 [53] Papageorgiou, G., Govindjee (Ed.), *Chlorophyll a Fluorescence - A*
49
50 *Signature of Photosynthesis*, Springer, Dordrecht 2004.
51
52
53
54
55
56
57
58
59
60

- 1
2
3
4
5
6 [54] Kitajima, M., Butler, W. L., Quenching of chlorophyll fluorescence and
7
8 primary photochemistry in chloroplasts by dibromothymoquinone. *Biochim.*
9
10 *Biophys. Acta* 1975, 376, 105-115.
11
12 [55] Schreiber, U., Chlorophyll fluorescence yield changes as a tool in plant
13
14 physiology. - I. The measuring system. *Photosynth. Res.* 1983, 4, 361-373.
15
16 [56] Meyer, S., Genty, B., Heterogeneous inhibition of photosynthesis over the
17
18 leaf surface of *Rosa rubiginosa* L. during water stress and abscisic acid treatment:
19
20 induction of a metabolic component by limitation of CO₂ diffusion. *Planta* 1999,
21
22 210, 126-131.
23
24 [57] Horton, P., Ruban, A. V., Walters, R. G., Regulation of light harvesting in
25
26 green plants. *Annu. Rev. Plant Physiol. Plant Molec. Biol.* 1996, 47, 655-684.
27
28 [58] Maxwell, K., Johnson, G. N., Chlorophyll fluorescence - a practical guide. *J.*
29
30 *Exp. Bot.* 2000, 51, 659-668.
31
32 [59] Gibbons, G. C., Smillie, R. M., Chlorophyll fluorescence photography to
33
34 detect mutants, chilling injury and heat stress. *Carlsberg Res. Commun.* 1980, 45,
35
36 269-282.
37
38 [60] Balota, M., Sowinska, M., Buschmann, C., Lichtenthaler, H.K., Heisel, F.,
39
40 Babani, F., Fluorescence techniques as suitable methods to discriminate wheat
41
42 genotypes under drought and high temperature condition. *Proc. SPIE* 1999, 3707,
43
44 103-113.
45
46 [61] Baker, N. R., Rosenqvist, E., Applications of chlorophyll fluorescence can
47
48 improve crop production strategies: an examination of future possibilities. *J. Exp.*
49
50 *Bot.* 2004, 55, 1607-1621.
51
52
53
54
55
56
57
58
59
60

- 1
2
3
4
5
6 [62] Daley, P. F., Chlorophyll fluorescence analysis and imaging in plant stress
7
8 and disease. *Can. J. Plant Pathol.* 1995, *17*, 167-173.
9
- 10 [63] Ning, L., Edwards, G. E., Strobel, G. A., Daley, L. S., Callis, J. B., Imaging
11
12 fluorometer to detect pathological and physiological change in plants. *Appl.*
13
14 *Spectrosc.* 1995, *49*, 1381-1389.
15
16
- 17 [64] Lichtenthaler, H. K., Lang, M., Sowinska, M., Heisel, F., Miede, J. A.,
18
19 Detection of vegetation stress via a new high resolution fluorescence imaging
20
21 system. *J. Plant Physiol.* 1996, *148*, 599-612.
22
23
- 24 [65] Buschmann, C., Lichtenthaler, H. K., Principles and characteristics of multi-
25
26 colour fluorescence imaging of plants. *J. Plant Physiol.* 1998, *152*, 297-314.
27
28
- 29 [66] Nedbal, L., Whitmarsh, J., Chlorophyll fluorescence imaging of leaves and
30
31 fruits, in: Papageorgiou, G. C., Govindjee (Ed.), *Chlorophyll a fluorescence: A*
32
33 *signature of photosynthesis*, Springer, Dordrecht 2004, pp. 389-407.
34
35
- 36 [67] Oxborough, K., Imaging of chlorophyll a fluorescence: theoretical and
37
38 practical aspects of an emerging technique for the monitoring of photosynthetic
39
40 performance. *J. Exp. Bot.* 2004, *55*, 1195-1205.
41
42
- 43 [68] Oxborough, K., Using chlorophyll a fluorescence imaging to monitor
44
45 photosynthetic performances, in: Papageorgiou, G. C., Govindjee (Ed.),
46
47 *Chlorophyll a Fluorescence: A Signature of Photosynthesis*, Springer, Dordrecht
48
49 2004, pp. 409-428.
50
51
- 52 [69] Lichtenthaler, H. K., Langsdorf, G., Lenk, S., Buschmann, C., Chlorophyll
53
54 fluorescence imaging of photosynthetic activity with the flash-lamp fluorescence
55
56 imaging system. *Photosynthetica* 2005, *43*, 355-369.
57
58
59
60

- 1
2
3
4
5
6 [70] Baker, N. R., Chlorophyll fluorescence: a probe of photosynthesis in vivo.
7
8 *Annu. Rev. Plant Biol.* 2008, 59, 89-113.
9
- 10 [71] Buschmann, C., Langsdorf, G., Lichtenthaler, H. K., The blue, green, red and
11
12 far-red fluorescence signatures of plant tissues, their multicolor fluorescence
13
14 imaging and application for agrofood assessment, in: Zude, M. (Ed.), *Optical*
15
16 *Methods for Monitoring Fresh and processed Food - Basics and Applications for*
17
18 *a better Understanding of non-destructive Sensing*, Taylor&Francis, CRC-Press,
19
20 Boca Raton 2008, pp. 272-319.
21
22
- 23 [72] Buschmann, C., Induction kinetics of heat emission before and after
24
25 photoinhibition in cotyledons of *Raphanus sativus*. *Photosynth. Res.* 1987, 14,
26
27 229-240.
28
29
- 30 [73] Osmond, B., Schwartz, O., Gunning, B., Photoinhibitory printing on leaves,
31
32 visualised by chlorophyll fluorescence imaging and confocal microscopy, is due
33
34 to diminished fluorescence from grana. *Aust. J. Plant Physiol.* 1999, 26, 717-724.
35
36
- 37 [74] Gray, G. R., Hope, B. J., Qin, X. Q., Taylor, B. G., Whitehead, C. L., The
38
39 characterization of photoinhibition and recovery during cold acclimation in
40
41 *Arabidopsis thaliana* using chlorophyll fluorescence imaging. *Physiol. Plant.*
42
43 2003, 119, 365-375.
44
45
- 46 [75] Lang, M., Lichtenthaler, H. K., Sowinska, M., Heisel, F., Miede, J. A.,
47
48 Fluorescence imaging of water and temperature stress in plant leaves. *J. Plant*
49
50 *Physiol.* 1996, 148, 613-621.
51
52
53
54
55
56
57
58
59
60

1
2
3
4
5
6 [76] Lenk, S., Buschmann, C., Distribution of UV-shielding of the epidermis of
7
8 sun and shade leaves of the beech (*Fagus sylvatica* L.) as monitored by multi-
9
10 colour fluorescence imaging. *J. Plant Physiol.* 2006, *163*, 1273-1283.

11
12 [77] Štroch, M., Lenk, S., Navrátil, M., Špunda, V., Buschmann, C., Epidermal
13
14 UV-shielding and photosystem II adjustment in wild type and *chlorina f2* mutant
15
16 of barley during exposure to increased PAR and UV radiation. *Environ. Exp. Bot.*
17
18 2008, *64*, 271-278.

19
20 [78] Krizek, D. T., Middleton, E. M., Sandhu, R. K., Kim, M. S., Evaluating UV-
21
22 B effects and EDU protection in cucumber leaves using fluorescence images and
23
24 fluorescence emission spectra. *J. Plant Physiol.* 2001, *158*, 41-53.

25
26 [79] Fryer, M. J., Ball, L., Oxborough, K., Karpinski, S., *et al.*, Control of
27
28 ascorbate peroxidase 2 expression by hydrogen peroxide and leaf water status
29
30 during excess light stress reveals a functional organisation of *Arabidopsis* leaves.
31
32 *Plant J.* 2003, *33*, 691-705.

33
34 [80] Fryer, M. J., Oxborough, K., Mullineaux, P. M., Baker, N. R., Imaging of
35
36 photo-oxidative stress responses in leaves. *J. Exp. Bot.* 2002, *53*, 1249-1254.

37
38 [81] Hideg, E., Schreiber, U., Parallel assessment of ROS formation and
39
40 photosynthesis in leaves by fluorescence imaging. *Photosynth. Res.* 2007, *92*,
41
42 103-108.

43
44 [82] Chang, C. C. C., Ball, L., Fryer, M. J., Baker, N. R., *et al.*, Induction of
45
46 ascorbate peroxidase 2 expression in wounded *Arabidopsis* leaves does not
47
48 involve known wound-signalling pathways but is associated with changes in
49
50 photosynthesis. *Plant J.* 2004, *38*, 499-511.
51
52
53
54
55
56
57
58
59
60

- 1
2
3
4
5
6 [83] Massacci, A., Jones, H. G., Use of simultaneous analysis of gas-exchange
7 and chlorophyll fluorescence quenching for analysing the effects of water stress
8 on photosynthesis in apple leaves. *Trees - Struct. Funct.* 1990, 4, 1-8.
9
10
11
12 [84] Barták, M., Hajek, J., Gloser, J., Heterogeneity of chlorophyll fluorescence
13 over thalli of several foliose macrolichens exposed to adverse environmental
14 factors: Interspecific differences as related to thallus hydration and high
15 irradiance. *Photosynthetica* 2000, 38, 531-537.
16
17
18 [85] Nejad, A. R., Harbinson, J., van Meeteren, U., Dynamics of spatial
19 heterogeneity of stomatal closure in *Tradescantia virginiana* altered by growth at
20 high relative air humidity. *J. Exp. Bot.* 2006, 57, 3669-3678.
21
22
23 [86] Georgieva, K., Lenk, S., Buschmann, C., Responses of the resurrection plant
24 *Haberlea rhodopensis* to high irradiance. *Photosynthetica* 2008, 46, 208-215.
25
26
27 [87] Osmond, C. B., Kramer, D., Luttge, U., Reversible, water stress-induced non-
28 uniform chlorophyll fluorescence quenching in wilting leaves of *Potentilla*
29 *reptans* may not be due to patchy stomatal responses. *Plant Biol.* 1999, 1, 618-
30 624.
31
32
33 [88] Lichtenthaler, H. K., Babani, F., Detection of photosynthetic activity and
34 water stress by imaging the red chlorophyll fluorescence. *Plant Physiol. Biochem.*
35 2000, 38, 889-895.
36
37
38 [89] Baker, N. R., Oxborough, K., Lawson, T., Morison, J. I. L., High resolution
39 imaging of photosynthetic activities of tissues, cells and chloroplasts in leaves. *J.*
40 *Exp. Bot.* 2001, 52, 615-621.
41
42
43
44
45
46
47
48
49
50
51
52
53
54
55
56
57
58
59
60

- 1
2
3
4
5
6 [90] Calatayud, A., Roca, D., Martinez, P. F., Spatial-temporal variations in rose
7 leaves under water stress conditions studied by chlorophyll fluorescence imaging.
8
9
10 *Plant Physiol. Biochem.* 2006, 44, 564-573.
11
- 12 [91] Heisel, F., Sowinska, M., Miehé, J. A., Lang, M., Lichtenthaler, H. K.,
13
14
15
16
17
18
19
20
21
22
23
24
25
26
27
28
29
30
31
32
33
34
35
36
37
38
39
40
41
42
43
44
45
46
47
48
49
50
51
52
53
54
55
56
57
58
59
60
- [92] Langsdorf, G., Buschmann, C., Sowinska, M., Babani, F., *et al.*, Multicolour
fluorescence imaging of sugar beet leaves with different nitrogen status by flash
lamp UV-excitation. *Photosynthetica* 2000, 38, 539-551.
- [93] Corp, L. A., McMurtrey, J. E., Middleton, E. M., Mulchi, C. L., *et al.*,
Fluorescence sensing systems: In vivo detection of biophysical variations in field
corn due to nitrogen supply. *Remote Sens. Environ.* 2003, 86, 470-479.
- [94] Cerovic, Z. G., Samson, G., Morales, F., Tremblay, N., Moya, I., Ultraviolet-
induced fluorescence for plant monitoring: present state and prospects. *Agronomie*
1999, 19, 543-578.
- [95] Buschmann, C., Variability and application of the chlorophyll fluorescence
emission ratio red/far-red of leaves. *Photosynth. Res.* 2007, 92, 261-271.
- [96] Omasa, K., Hashimoto, Y., Aiga, I., A quantitative analysis of the
relationships between SO₂ or NO₂ sorption and their acute effects on plant leaves
using image instrumentation. *Environ. Contr. Biol.* 1981, 19, 59-67.
- [97] Omasa, K., Hashimoto, Y., Aiga, I., A quantitative analysis of the
relationships between O₃ sorption and its acute effects on plant leaves using image
instrumentation. *Environ. Contr. Biol.* 1981, 19, 85-92.

- 1
2
3
4
5
6 [98] Valcke, R., Ciscato, M., Heisel, F., Miehé, J., Sowinska, M., Analysis of
7 heavy metal stressed plants by fluorescence imaging. *Proceedings of SPIE - Laser*
8 *Radar Technology and Applications IV* 1999, 3707, 82-90.
9
10
11
12 [99] Gielen, B., Vandermeiren, K., Horemans, N., D'Haese, D., *et al.*, Chlorophyll
13 a fluorescence imaging of ozone-stressed *Brassica napus* L. plants differing in
14 glucosinolate concentrations. *Plant Biol.* 2006, 8, 698-705.
15
16
17 [100] Gielen, B., Low, M., Deckmyn, G., Metzger, U., *et al.*, Chronic ozone
18 exposure affects leaf senescence of adult beech trees: a chlorophyll fluorescence
19 approach. *J. Exp. Bot.* 2007, 58, 785-795.
20
21
22 [101] Leipner, J., Oxborough, K., Baker, N. R., Primary sites of ozone-induced
23 perturbations of photosynthesis in leaves: identification and characterization in
24 *Phaseolus vulgaris* using high resolution chlorophyll fluorescence imaging. *J.*
25 *Exp. Bot.* 2001, 52, 1689-1696.
26
27
28 [102] Kim, M. S., McMurtrey, J. E., Mulchi, C. L., Daughtry, C. S. T., *et al.*,
29 Steady-state multispectral fluorescence imaging system for plant leaves. *Appl.*
30 *Opt.* 2001, 40, 157-166.
31
32
33 [103] Chaerle, L., Hagenbeek, D., Vanrobaeys, X., Van Der Straeten, D., Early
34 detection of nutrient and biotic stress in *Phaseolus vulgaris*. *Int. J. Remote Sens.*
35 2007, 29, 3479-3492.
36
37
38 [104] Quilliam, R. S., Swarbrick, P. J., Scholes, J. D., Rolfe, S. A., Imaging
39 photosynthesis in wounded leaves of *Arabidopsis thaliana*. *J. Exp. Bot.* 2006, 57,
40 55-69.
41
42
43
44
45
46
47
48
49
50
51
52
53
54
55
56
57
58
59
60

- 1
2
3
4
5
6 [105] Yanase, D., Andoh, A., Translocation of photosynthesis - inhibiting
7 herbicides in wheat leaves measured by phytofluorography, the chlorophyll
8 fluorescence imaging. *Pest. Biochem. Physiol.* 1992, *44*, 60-67.
9
10
11
12 [106] Lichtenthaler, H. K., Lang, M., Sowinska, M., Summ, P., *et al.*, Uptake of
13 the herbicide diuron as visualised by the fluorescence imaging technique. *Bot.*
14 *Acta* 1997, *110*, 158-163.
15
16
17 [107] Hulsen, K., Top, E. M., Hofte, M., Biodegradation of linuron in a *Phaseolus*
18 bioassay detected by chlorophyll fluorescence. *New Phytol.* 2002, *154*, 821-829.
19
20
21 [108] Kim, J.-H., Jung, J.-E., Lee, C.-H., *In vivo* monitoring of the incorporation
22 of chemicals into cucumber and rice leaves by chlorophyll fluorescence imaging.
23 *Korean J. Plant Biotechnol.* 2002, *4*, 173-179.
24
25
26 [109] Barbagallo, R. P., Oxborough, K., Pallett, K. E., Baker, N. R., Rapid,
27 noninvasive screening for perturbations of metabolism and plant growth using
28 chlorophyll fluorescence Imaging. *Plant Physiol.* 2003, *132*, 485-493.
29
30
31 [110] Tang, J. Y., Zielinski, R. E., Zangerl, A. R., Crofts, A. R., *et al.*, The
32 differential effects of herbivory by first and fourth instars of *Trichoplusia ni*
33 (Lepidoptera: Noctuidae) on photosynthesis in *Arabidopsis thaliana*. *J. Exp. Bot.*
34 2006, *57*, 527-536.
35
36
37 [111] Zangerl, A. R., Hamilton, J. G., Miller, T. J., Crofts, A. R., *et al.*, Impact of
38 folivory on photosynthesis is greater than the sum of its holes. *Proc. Natl. Acad.*
39 *Sci. U.S.A.* 2002, *99*, 1088-1091.
40
41
42 [112] Bown, A. W., Hall, D. E., MacGregor, K. B., Insect footsteps on leaves
43 stimulate the accumulation of 4-aminobutyrate and can be visualized through
44
45
46
47
48
49
50
51
52
53
54
55
56
57
58
59
60

1
2
3
4
5
6 increased chlorophyll fluorescence and superoxide production *Plant Physiol.*

7
8 2002, *129*, 1430-1434.

9
10 [113] Schmitz, A., Tartachnyk, II, Kiewnick, S., Sikora, R. A., Kuhbauch, W.,

11
12 Detection of *Heterodera schachdi* infestation in sugar beet by means of laser-

13
14 induced and pulse amplitude modulated chlorophyll fluorescence. *Nematology*

15
16 2006, *8*, 273-286.

17
18 [114] Bonfig, K. B., Schreiber, U., Gabler, A., Roitsch, T., Berger, S., Infection

19
20 with virulent and avirulent *P. syringae* strains differentially affects photosynthesis

21
22 and sink metabolism in *Arabidopsis* leaves. *Planta* 2006, *225*, 1-12.

23
24 [115] Berger, S., Benediktyova, Z., Matous, K., Bonfig, K., *et al.*, Visualization of

25
26 dynamics of plant-pathogen interaction by novel combination of chlorophyll

27
28 fluorescence imaging and statistical analysis: differential effects of virulent and

29
30 avirulent strains of *P. syringae* and of oxylipins on *A. thaliana*. *J. Exp. Bot.* 2007,

31
32 58, 797-806.

33
34 [116] Rodríguez-Moreno, L., Pineda, M., Soukupová, J., Macho, A. P., *et al.*,

35
36 Early detection of bean infection by *Pseudomonas syringae* in asymptomatic leaf

37
38 areas using chlorophyll fluorescence imaging. *Photosynth. Res.* 2006, *96*, 27-35.

39
40 [117] Matouš, K., Benediktyova, Z., Berger, S., Roitsch, T., Nedbal, L., Case

41
42 study of combinatorial imaging: What protocol and what chlorophyll fluorescence

43
44 image to use when visualizing infection of *Arabidopsis thaliana* by *Pseudomonas*

45
46 *syringae*? *Photosynth. Res.* 2006, *90*, 243-253.

- 1
2
3
4
5
6 [118] Szigeti, Z., Almási, A., Sárvári, E., Changes in the photosynthetic function
7
8 in leaves of Chinese cabbage infected with turnip yellow mosaic virus. *Acta*
9
10 *Biologica Szegediensis* 2002, 46, 137-138.
11
- 12 [119] Chaerle, L., Lenk, S., Hagenbeek, D., Buschmann, C., Van Der Straeten, D.,
13
14 Multicolor fluorescence imaging for early detection of the hypersensitive reaction
15
16 to tobacco mosaic virus. *J. Plant Physiol.* 2007, 164, 253-262.
17
18
- 19 [120] Balachandran, S., Osmond, C. B., Daley, P. F., Diagnosis of the earliest
20
21 strain-specific interactions between tobacco mosaic virus and chloroplasts of
22
23 tobacco leaves *in vivo* by means of chlorophyll fluorescence imaging. *Plant*
24
25 *Physiol.* 1994, 104, 1059-1065.
26
27
- 28 [121] Osmond, C. B., Daley, P. F., Badger, M. R., Lüttge, U., Chlorophyll
29
30 fluorescence quenching during photosynthetic induction in leaves of *Abutilon*
31
32 *striatum* Dicks. infected with abutilon mosaic virus, observed with a field-portable
33
34 imaging system. *Bot. Acta* 1998, 111, 390-397.
35
36
- 37 [122] Lohaus, G., Heldt, H. W., Osmond, C. B., Infection with phloem limited
38
39 abutilon mosaic virus causes localized carbohydrate accumulation in leaves of
40
41 *Abutilon striatum*: Relationships to symptom development and effects on
42
43 chlorophyll fluorescence quenching during photosynthetic induction. *Plant Biol.*
44
45 2000, 2, 161-167.
46
47
- 48 [123] Pérez-Bueno, M., Ciscato, M., vandeVen, M., García-Luque, I., *et al.*,
49
50 Imaging viral infection: studies on *Nicotiana benthamiana* plants infected with the
51
52 pepper mild mottle tobamovirus. *Photosynth. Res.* 2006, 90, 111-123.
53
54
55
56
57
58
59
60

- 1
2
3
4
5
6 [124] Meyer, S., Saccardy-Adji, K., Rizza, F., Genty, B., Inhibition of
7
8 photosynthesis by *Colletotrichum lindemuthianum* in bean leaves determined by
9
10 chlorophyll fluorescence imaging. *Plant Cell Environ.* 2001, 24, 947-955.
11
12 [125] Berger, S., Papadopoulos, M., Schreiber, U., Kaiser, W., Roitsch, T.,
13
14 Complex regulation of gene expression, photosynthesis and sugar levels by
15
16 pathogen infection in tomato. *Physiol. Plant.* 2004, 122, 419-428.
17
18 [126] Swarbrick, P. J., Schulze-Lefert, P., Scholes, J. D., Metabolic consequences
19
20 of susceptibility and resistance (race-specific and broad-spectrum) in barley
21
22 leaves challenged with powdery mildew. *Plant Cell Environ.* 2006, 29, 1061-
23
24 1076.
25
26 [127] Scharte, J., Schon, H., Weis, E., Photosynthesis and carbohydrate
27
28 metabolism in tobacco leaves during an incompatible interaction with
29
30 *Phytophthora nicotianae*. *Plant Cell Environ.* 2005, 28, 1421-1435.
31
32 [128] Bélanger, M. C., Roger, J. M., Cartolaro, P., Viau, A. A., Bellon-Maurel,
33
34 V., Detection of powdery mildew in grapevine using remotely sensed UV-induced
35
36 fluorescence. *Int. J. Remote Sens.* 2008, 29, 1707-1724.
37
38 [129] Bowyer, W. J., Ning, L., Daley, L. S., Strobel, G. A., *et al.*, In vivo
39
40 fluorescence imaging for detection of damage to leaves by fungal phytotoxins.
41
42 *Spectroscopy* 1998, 13, 36-44.
43
44 [130] Soukupova, J., Smatanova, S., Nedbal, L., Jegorov, A., Plant response to
45
46 destruxins visualized by imaging of chlorophyll fluorescence. *Physiol. Plant.*
47
48 2003, 118, 399-405.
49
50
51
52
53
54
55
56
57
58
59
60

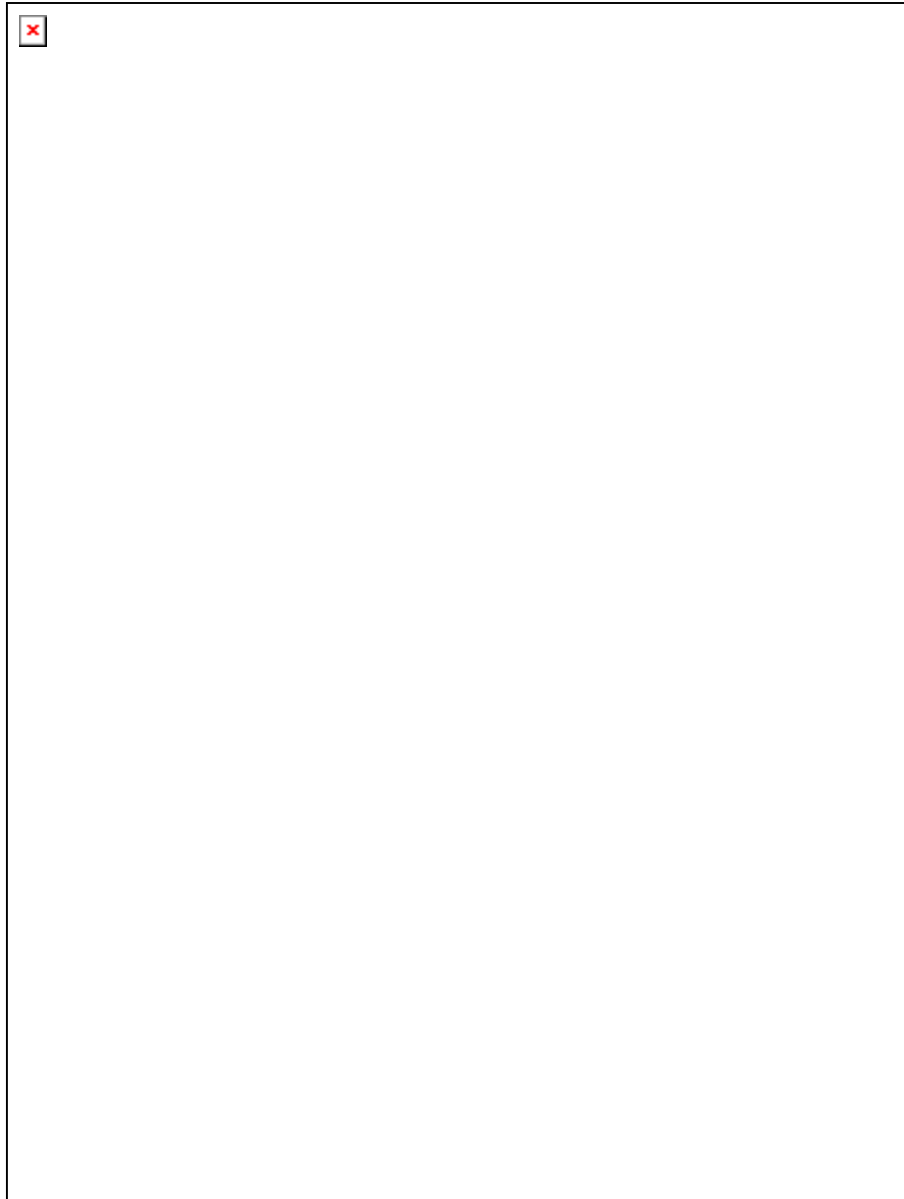
- 1
2
3
4
5
6 [131] Scholes, J. D., Rolfe, S. A., Photosynthesis in localised regions of oat leaves
7
8 infected with crown rust (*Puccinia coronata*): quantitative imaging of chlorophyll
9
10 fluorescence. *Planta* 1996, *199*, 573-582.
11
- 12 [132] Peterson, R. B., Aylor, D. E., Chlorophyll fluorescence induction in leaves
13
14 of *Phaseolus vulgaris* infected with bean rust (*Uromyces appendiculatus*). *Plant*
15
16 *Physiol.* 1995, *108*, 163-171.
17
- 18 [133] Polder, G., van der Heijden, G. W. A. M., Jalink, H., Snel, J. F. H.,
19
20 Correcting and matching time sequence images of plant leaves using Penalized
21
22 Likelihood Warping and Robust Point Matching. *Comput. Electron. Agric.* 2007,
23
24 55, 1-15.
25
26
27
28
- 29 [134] Moller, M., Alchanatis, V., Cohen, Y., Meron, M., *et al.*, Use of thermal and
30
31 visible imagery for estimating crop water status of irrigated grapevine. *J. Exp.*
32
33 *Bot.* 2007, *58*, 827-838.
34
- 35 [135] West, J. D., Peak, D., Peterson, J. Q., Mott, K. A., Dynamics of stomatal
36
37 patches for a single surface of *Xanthium strumarium* L. leaves observed with
38
39 fluorescence and thermal images. *Plant Cell Environ.* 2005, *28*, 633-641.
40
41
- 42 [136] Kana, R., Vass, I., Thermoimaging as a tool for studying light-induced
43
44 heating of leaves Correlation of heat dissipation with the efficiency of
45
46 photosystem II photochemistry and non-photochemical quenching. *Environ. Exp.*
47
48 *Bot.* 2008, *64*, 90-96.
49
50
- 51 [137] Hideg, E., Juhasz, M., Bornman, J. F., Asada, K., The distribution and
52
53 possible origin of blue-green fluorescence in control and stressed barley leaves.
54
55
56
57 *Photochem. Photobiol. Sci.* 2002, *1*, 934-941.
58
59
60

1
2
3
4
5
6 [138] Hideg, E., Barta, C., Kalai, T., Vass, I., *et al.*, Detection of singlet oxygen
7
8 and superoxide with fluorescent sensors in leaves under stress by photoinhibition
9
10 or UV radiation. *Plant Cell Physiol.* 2002, 43, 1154-1164.

11
12 [139] Hogewoning, S. W., Harbinson, J., Insights on the development, kinetics,
13
14 and variation of photoinhibition using chlorophyll fluorescence imaging of a
15
16 chilled, variegated leaf. *J. Exp. Bot.* 2007, 58, 453-463.

17
18 [140] Chaerle, L., vande Ven, M., Valcke, R., Van Der Straeten, D., Visualisation
19
20 of early stress responses in plant leaves. *Proc. SPIE* 2002, 4710, 417-423.

21
22 [141] Boccara, M., Boue, C., Garmier, M., De Paepe, R., Boccara, A. C., Infra-red
23
24 thermography revealed a role for mitochondria in pre-symptomatic cooling
25
26 during harpin-induced hypersensitive response. *Plant J.* 2001, 28, 663-670.
27
28
29
30
31
32
33
34
35
36
37
38
39
40
41
42
43
44
45
46
47
48
49
50
51
52
53
54
55
56
57
58
59
60



Comparison of presymptomatic symptoms of 3 plant pathogen interactions. Each column displays from top to bottom visual colour image, thermal image and chlorophyll fluorescence image at respectively low and high excitation intensity.

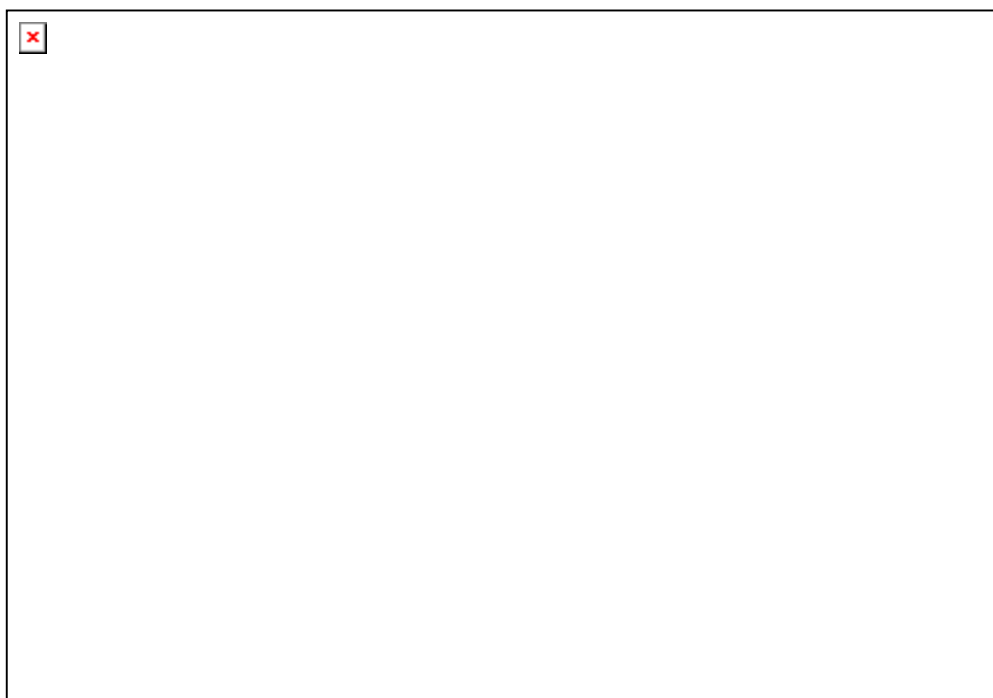
Left column: 54 hours after infection, the TMV-tobacco (*Nicotiana tabacum*) interaction results in a local temperature increase (second row), beyond the visually affected area (image first row). The area of chlorophyll fluorescence decrease is also more extended than the visual damage, and expanding further outward is a halo of increased fluorescence (third row). Chlorophyll fluorescence under high intensity illumination only show the extent of tissue death (fourth row) (see also [46]). Middle column: *Cercospora beticola* infection of sugar beet (*Beta vulgaris*) at 7 days after infection shows a local decrease in leaf temperature (second row), while the visual effect is limited to a pin-point lesion (first row), which can also be seen as a small spot of lower chlorophyll fluorescence (third row). An increase in chlorophyll fluorescence is visible around this spot, and is more clearly visible at higher intensity illumination (fourth row) (see also [46]).

1
2
3 Right column: *Botrytis cinerea* infection of common bean (*Phaseolus vulgaris*) 21 h after infection.

4 An increase in local, leaf temperature is apparent (second row), while a few co-located spots of
5 increased chlorophyll fluorescence are detectable (third row). As a reference a wounding spot is
6 included on the other side of the main leaf vein, and visible as a cold spot in the thermal picture
7 (second row). The visible damage (first row) corresponds to the black spots in the Chl-F image
8 captured at high light-intensity (fourth row) (see also [102]).
9

10 262x345mm (72 x 72 DPI)
11
12
13
14
15
16
17
18
19
20
21
22
23
24
25
26
27
28
29
30
31
32
33
34
35
36
37
38
39
40
41
42
43
44
45
46
47
48
49
50
51
52
53
54
55
56
57
58
59
60

For Peer Review



Arabidopsis plants as imaged with a multispectral fluorescence imaging system. In each panel, upper left and lower right position feature a spontaneous cell death mutant lsd (lesions simulating disease resistance, [42]; the other 2 plants are the Col-0 wild type from which this mutant was derived. Upper left: color reflectance image, middle panel: green fluorescence emission (550nm), right panel: chlorophyll fluorescence emission (690nm). The lower panels show thresholding of respectively color video and green fluorescence image, the latter indicating the leaf area affected by cell death. Thresholding of the chlorophyll fluorescence image includes part of the growing medium background and displays little or no contrast between affected and unaffected leaf areas, as is already evident from the depicted original fluorescence image. The lower right panel shows a

schematic robotized system applicable for multi-sensor imaging.

254x176mm (72 x 72 DPI)

